

Translation symmetry restoration in integrable systems: the noninteracting case

Molly Gibbins,^{1,2} Adam Gammon-Smith,^{1,2} and Bruno Bertini³

¹*School of Physics and Astronomy, University of Nottingham, Nottingham, NG7 2RD, UK*

²*Centre for the Mathematics and Theoretical Physics of Quantum Non-Equilibrium Systems, University of Nottingham, Nottingham, NG7 2RD, UK*

³*School of Physics and Astronomy, University of Birmingham, Birmingham, B15 2TT*

(Dated: June 18, 2025)

The study of symmetry restoration has recently emerged as a fruitful means to extract high-level information on the relaxation of quantum many-body systems. This revealed, for instance, the surprising ‘quantum Mpemba effect’ that occurs when a symmetry is restored more rapidly when the initial configuration is less symmetric. While the restoration of internal symmetries has been investigated intensively, however, the one of spatial symmetries has only been considered recently in the context of random unitary circuits. Here we present a complementary study of translation symmetry restoration in integrable systems. Specifically, we consider non-interacting spinless fermions on the lattice prepared in non-equilibrium states invariant only under $\nu > 1$ lattice shifts and follow the restoration of one-site shift invariance. We do so by measuring the Frobenius distance between the state on a subsystem, and its symmetrised counterpart. We compute the latter exactly, using standard Gaussian methods, and formulate a quasiparticle picture — involving multiplets of ν correlated quasiparticles — to describe analytically its asymptotic behaviour. We show that, differently from random unitary circuits where symmetry restoration occurs abruptly for times proportional to the subsystem size, here symmetry is restored smoothly and over timescales of the order of the subsystem size squared. Interestingly, we also show that, in contrast to the case of continuous internal symmetries, the quasiparticle picture does not provide a quantitative description of discrete translation symmetry restoration and that the latter process goes beyond the hydrodynamic description. Our results can directly be extended to higher dimensions.

Introduction.— Studying the dynamics of quantum many-body systems is often complicated by the fact that local observables generate specific artifacts that are hard to filter out. Recent research has shown that a convenient way to circumvent this problem is to study the restoration of the symmetries of the dynamics that are broken by the initial state. Indeed, the latter process can be characterised in a direct and observable-independent way by measuring the distance between the state of a local subsystem and its symmetrised version [1]. This revealed, for instance, a surprising phenomenon connected with the equilibration process that was not pointed out before: sometimes the symmetry is restored faster when the initial state is less symmetric. This effect bears a conceptual similarity with the Mpemba effect [2], occurring when warmer water freezes faster than colder one, and has been accordingly dubbed the quantum Mpemba effect (QME) [1, 3]. Since its first observation, the QME has been theoretically predicted to occur in many different classes of systems ranging from integrable (free and interacting) [4–18] to strongly non-integrable [19–22] systems and even observed in trapped ion quantum simulators [23].

Despite the intense research on the subject, most of the studies conducted so far have considered the restoration of internal symmetries — $U(1)$ symmetries in the vast majority of the cases. This restriction comes for a technical, rather than conceptual, reason: these symmetries generate particularly simple charges and this simplifies the analysis. Studying the restoration of other kinds of symmetries, however, can drastically widen the scope of this line of research. For instance, spatial symmetries are

arguably a more generic feature of quantum many-body systems than internal ones. In this context, the study of spatial symmetry restoration has been initiated, and so far only considered, in Ref. [21], which focussed on a class of ergodic (quantum chaotic) quantum systems — random unitary circuits — demonstrating the occurrence of QME for intermediate sizes. Here we complement this study by considering translation symmetry restoration in integrable systems under constant Hamiltonian evolution. In fact, for the sake of simplicity, we focus on a simple non-interacting case.

More specifically, we consider an infinite (or periodic) one-dimensional chain of spinless fermions on the lattice, whose dynamics are described by the tight binding Hamiltonian

$$H_{\text{TB}} = \sum_j (c_j^\dagger c_{j+1} + \text{h.c.}). \quad (1)$$

Although this Hamiltonian is invariant under single-site translations — $[H_{\text{TB}}, T] = 0$, where T is the translation operator $T c_j T^{-1} = c_{j+1}$ — we consider initial states that are only invariant under ν -site shifts. Specifically, we consider product states of the form $|\Psi\rangle = \otimes_j |\Psi_\nu\rangle$, where $|\Psi_\nu\rangle$ is a Gaussian state defined on ν sites. The dynamics of the tight-binding model from states of this kind were recently considered in Ref. [24], which studied lattices of arbitrary dimension $d \geq 1$. Our upcoming discussion can be similarly generalised to higher dimensions.

Following Ref. [21], to study the breaking and local restoration of the translation symmetry in a subsystem A (of length l), we use the Frobenius distance between

the reduced density matrix $\rho_A(t)$ and the reduced symmetrised state defined as

$$\bar{\rho}_A(t) = \frac{1}{\nu} \sum_{j=0}^{\nu-1} \rho_A^{(j)}(t), \quad \rho_A^{(j)}(t) \equiv \text{tr}_{\bar{A}}(T^j \rho(t) T^{-j}), \quad (2)$$

where $\rho(t) = |\Psi_t\rangle\langle\Psi_t|$ is the state of the system at time t . Our figure of merit — the *Frobenius distance* between the reduced density matrix and its symmetrized counterpart — is defined as

$$\Delta F_A(t) \equiv \frac{\|\rho_A(t) - \bar{\rho}_A(t)\|}{\|\rho_A(t)\|}, \quad (3)$$

where $\|A\| \equiv \sqrt{\text{tr}(AA^\dagger)}$ is the Frobenius norm and $\rho_A = \text{tr}_{\bar{A}}(\rho)$ is the reduced density matrix. As discussed in Ref. [21], when studying the restoration of spatial symmetries Eq. (3) is more convenient than the entanglement asymmetry introduced in Ref. [1] because the latter is much harder to access analytically. In our case, however, the two quantities become equivalent at leading order in t and l [25].

Exact dynamics.— The dynamics of $\Delta F_A(t)$ can be computed exactly by exploiting the Gaussianity of the initial state and of the dynamics, which allow us to write the Frobenius distance in terms of determinants of $l \times l$ matrices in the presence of number conservation [25]. For instance, in Fig. 1 we present the translation symmetry restoration in two families of states

$$\begin{aligned} |\psi_2(\lambda_2)\rangle &= \prod \frac{(c_{2j}^\dagger + \lambda_2 c_{1+2j}^\dagger)}{\sqrt{1 + \lambda_2^2}} |0\rangle, \\ |\psi_4(\lambda_4)\rangle &= \prod c_{4j}^\dagger \frac{(c_{2+4j}^\dagger + \lambda_4 c_{1+4j}^\dagger)}{\sqrt{1 + \lambda_4^2}} |0\rangle. \end{aligned} \quad (4)$$

Interestingly, we see that the Frobenius distance decays as a power law in time in the asymptotic limit. This is in contrast with the sharp, initial-state-independent restoration at $t \propto l$ observed in random unitary circuits [21]. Moreover, the figure displays two distinct cases where QME is observed, indicated by the shaded orange boxes. The later crossing occurs between an instance of $|\psi_2(\lambda_2)\rangle$ and one of $|\psi_4(\lambda_4)\rangle$, explicitly involving two states with two different ‘levels’ of initial symmetry breaking. The earlier crossing occurs between two instances of $|\psi_4(\lambda_4)\rangle$, and the amount of symmetry breaking is implicitly controlled by the superposition parameter λ_4 . However, this figure also demonstrates that QME is does not always occur, and for instance, is not observed for $\lambda_2 = 0.15$ and $\lambda_4 = 0.1$.

Quasiparticle Picture.— In many cases the asymptotic dynamics (at large scales) of free-fermions can be described by the quasiparticle picture à la Calabrese and Cardy [26]. The intuition behind this picture is that in non-interacting systems (and more generally in interacting integrable ones) the large-scale dynamics can be described in terms of the motion of stable quasiparticles created by the initial state (which is highly excited with respect to the time-evolving Hamiltonian) that move as free

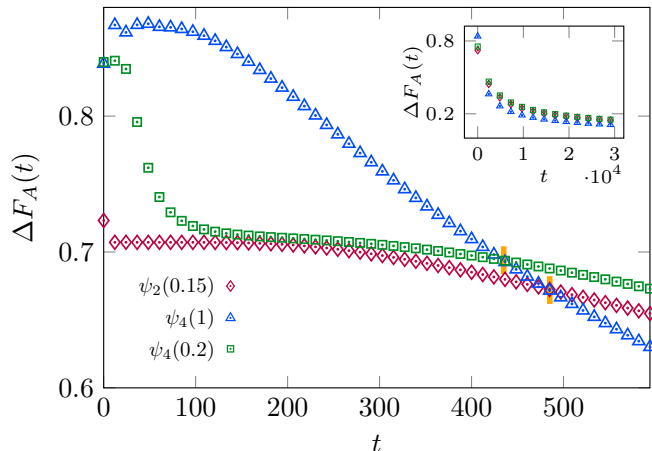


FIG. 1. The Frobenius distance $\Delta F_A(t)$, obtained via exact diagonalisation using Gaussian methods for subsystem size $l = 100$ and different initial states. The states are of the form $|\psi_\nu(\lambda)\rangle$ where ν is the translational invariance and λ is the superposition parameter, and their exact definitions are given in Eq. (4). Crossings between the Frobenius distance of different states, which correspond to instances of the quantum Mpemba effect, are indicated by the shaded orange boxes. *Inset:* Main plot extended to late times, showing that no further crossings occur.

classical particles with fixed velocity. The correlations among the quasiparticles are generated by the initial state but, crucially, *not by the dynamics*. This reduces the calculation of the time evolution of relevant quantities to an exercise of simple kinematics. Note that for Gaussian systems as those under consideration here, the quasiparticle picture can be derived through an asymptotic expansion of the relevant determinants [14, 27]. This picture successfully captures the dynamics of entanglement growth [26–29], as well as the QME for internal symmetries [1, 14]. Here we develop a similar approach to describe the asymptotic behaviour of $\Delta F_A(t)$ in the case of translation symmetry restoration.

In our case the quasiparticles are nothing but a semiclassical version of the momentum modes, therefore, their velocities are given by $v(k) = \epsilon'(k) = -2 \sin(k)$, where $\epsilon(k) = \cos(k)$ is the dispersion relation of the Hamiltonian in Eq. (1). In order to assign them well-defined positions we operate at an ‘intermediate resolution’: we divide space into unit cells of size δ satisfying $a \ll \delta \ll l$ — where a is the lattice spacing — and perform a *partial Fourier transform* of the initial state within each cell [24, 30]. This approach becomes particularly useful when the initial correlations are confined to small, regular groups of quasiparticles. This is the case for us as the translational symmetry of the initial state confers a ν -plet structure to these correlations [24]. More precisely, a given mode in the reduced Brillouin zone $k \in [0, 2\pi/\nu)$ is correlated only with those from the same cell with $k' \in \{k + 2\pi/\nu, k + 4\pi/\nu, \dots, k + 2(\nu - 1)\pi/\nu\}$. We sometimes refer to these correlated modes as ‘cell

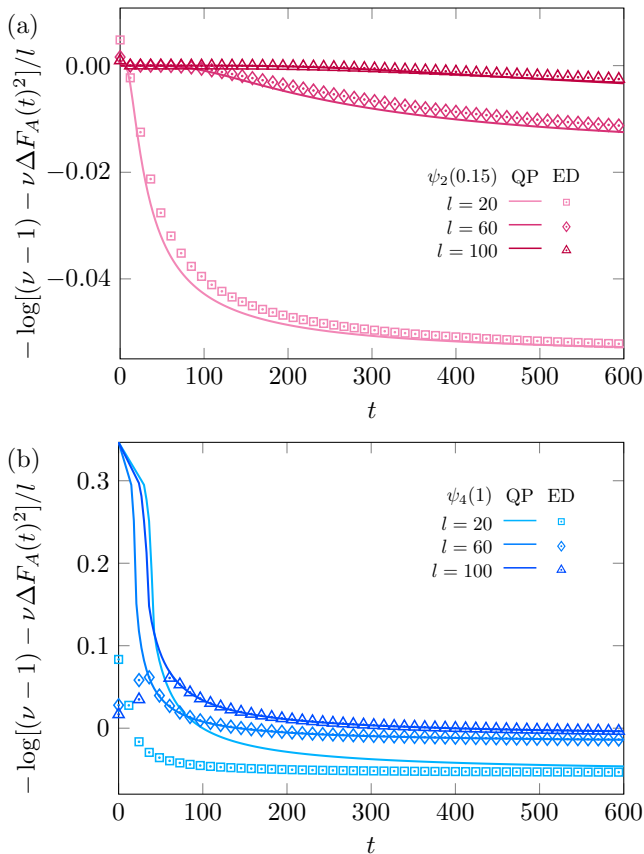


FIG. 2. Comparison of exact diagonalisation (data points) and quasiparticle method (solid lines) for $-\log[(\nu - 1) - \nu \Delta F_A(t)^2]/l$ as subsystem size is increased. Each panel focuses on a different state, (a) $\psi_2(0.15)$ and (b) $\psi_4(1)$, respectively.

modes’.

In summary, we assume that the quench generates ν -plets in localised in cells of size $\Delta \ll l$ and their full evolution can therefore be classically determined. This allows us to write the following semiclassical representation of the time evolved state [24, 30]

$$\rho_A(t) = \bigotimes_{x \in \mathbb{Z}_{L/\Delta}} \bigotimes_{p \in \frac{2\pi}{\Delta} \mathbb{Z}_{\Delta/\nu}} \rho_A(x, p), \quad (5)$$

where $\rho_A(x, p)$ is given in terms of the *semiclassical modes*

$$c_{x,p} = \frac{1}{\sqrt{\Delta}} \sum_{n \in \mathbb{Z}_{\Delta}^d} e^{ipn} c_{\Delta x + n}, \quad p \in \frac{2\pi}{\Delta} \mathbb{Z}_{\Delta}^d. \quad (6)$$

More precisely, $\rho_A(x, p)$ is formed by considering each ν -plet of correlated modes produced by the initial state tracing out all those that are out of the subsystem A at time t [24]. Note that, because $|\Psi_0\rangle$ is Gaussian, the correlations involving $\rho_A(x, p)$ can be computed from the (single-particle) *correlation matrix*

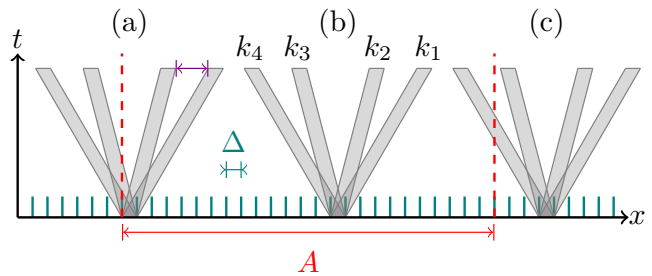


FIG. 3. Different cell mode bipartitions for a $\nu = 4$ initial state with respect to subsystem A . The multiplet is produced in a unit cell of size Δ and each cell mode $k_n(p) = p + 2\pi n/\nu$ propagates with fixed velocity $v_n(p) = 2 \sin(p + 2\pi n/\nu)$. (a) A bipartition in which two cell modes are inside the subsystem. The purple dimension line indicates a *relative velocity* between adjacent modes, which will be important for later discussion. (b) The bipartition in which all cell modes are inside the subsystem. This contributes to the Frobenius distance but not to the entanglement entropy. (c) A bipartition in which one cell mode is inside the subsystem. This contributes to the entanglement entropy but not to the Frobenius distance.

$$[C_A(x, p)]_{k,k'} \equiv \text{tr} \left(\rho_A(x, p) \hat{c}_{(x,p+k)}^\dagger \hat{c}_{(x,p+k')} \right). \quad (7)$$

To compute the Frobenius distance in Eq. (3) we treat $\rho_A^{(j)}(t)$ (cf. Eq. (2)), by writing them as in Eq. (5) with $\rho_A(x, p)$ replaced by $\rho_A^{(j)}(x, k) = T_A^j \rho_A(x, p) T_A^{-j}$, where T_A is the periodic one-site translation operator in the subsystem A [31]. This eventually gives us [25]

$$\Delta F_A(t)|_{\text{QP}} = \sqrt{\frac{(\nu - 1)}{\nu} - \frac{1}{\nu} \sum_{j=1}^{\nu-1} r_A^{(j)}(t)}, \quad (8)$$

where we set

$$r_A^{(j)}(t) = \exp \left[\int_{A \times [0, \frac{2\pi}{\nu}]} \frac{dx dk}{2\pi} \log \frac{\text{tr} [\rho_A(x, k) \rho_A^{(j)}(x, k)]}{\text{tr} [\rho_A^2(x, k)]} \right]. \quad (9)$$

Two interesting comments are in order concerning this expression.

First, although Eqs. (8) and (9) allow one to compute the Frobenius distance by establishing how multiplets of correlated quasiparticles are split between A and \bar{A} , the contributions controlling symmetry restoration differ from those controlling the saturation of spatial entanglement [26]. Indeed, while bipartitions where one single quasiparticle is either in or out of the system, e.g. Fig. 3 (a), contribute to the spreading of entanglement, they do not contribute to Eqs. (8) and (9). Instead, it is the bipartitions with exactly two modes inside the subsystem, e.g. Fig. 3 (c), which determine the asymptotic behaviour of the Frobenius distance. Noting that the former bipartitions are the only ones surviving at late times, and are

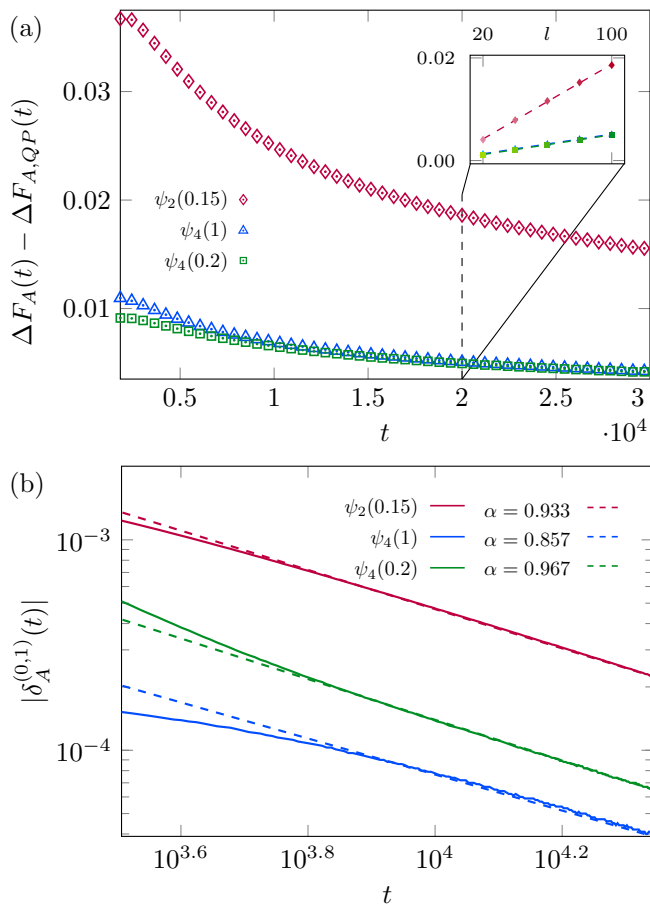


FIG. 4. (a) The difference between exact diagonalisation and quasiparticle solutions to the Frobenius distance, $\Delta F_A(t) - \Delta F_{A,QP}(t)$, for different initial states and subsystem size $l = 100$. (b) The leading non-extensive correction $\delta_A^{(0,1)}(t)$, defined in Eq. (11), for each of these initial states and subsystem size $l = 200$. This panel is displayed on log-log scale at late times only, and the slopes of the dashed lines approximate the decay of the correction at large times as $t^{-\alpha}$. *Inset (a)*: Example, shown for $t = 20000$, of the linear scaling of the difference $\Delta F_A(t) - \Delta F_{A,QP}(t)$ with system size.

those characterising the hydrodynamic regime where the state of the subsystem is locally stationary [32–34], we conclude that — even when studied within the quasiparticle picture — the symmetry restoration goes beyond hydrodynamics.

Second, Eq. (8) involves two further approximations in addition to the basic quasiparticle picture: (i) In the definition of $\rho_A^{(j)}(x, k)$ we applied the translation only to the subsystem of interest. In other words, we assumed

$$\text{tr}\left(\rho_A^{(i)}(t)\rho_A^{(j)}(t)\right) \simeq \text{tr}\left(\rho_A(t)T_A^{j-i}\rho_A(t)T_A^{i-j}\right), \quad (10)$$

where \simeq denotes equality at leading order in the subsystem size. This amounts to neglecting the boundary terms induced by a *full-system* translation of the *partial* Fourier creation operator. (ii) We computed the logarithm of the r.h.s. of Eq. (10) using the quasiparticle

picture. Although one can rigorously show that this correctly accounts for the leading order in the subsystem size [14, 27], there are generically non-extensive corrections that we neglected. This step is inoffensive in the case of continuous symmetries, see, e.g., Ref. [3, 4, 11, 14], where the leading contribution to $\Delta F_A(t)$ comes from terms where $i - j$ is infinitesimal. The discrete summation in Eq. (8), however, only involves terms with finite $i - j$ and forces us to reconsider this point.

Concerning (i), we find that Eq. (10) does indeed hold, with our results reported in Fig. 2 demonstrating a rapid convergence of the extensive part of the results obtained via exact diagonalisation (ED) to the quasiparticle (QP) prediction for increasing subsystem size. The innocent-looking neglect of non-extensive terms (ii), however, leads to substantial disagreements between ED and QP that appear to worsen for increasing values of l , see, e.g., the first panel of Fig 4. This can be understood by noting that the corrections

$$\delta_A^{(i,j)}(t) = \log \frac{\text{tr}\left(\rho_A^{(i)}(t)\rho_A^{(j)}(t)\right)}{\text{tr}\left(\rho_A^{(0)}(t)^2\right)} - \log r_A^{(j-i)}(t), \quad (11)$$

generate non-trivial coefficients for the terms in the sum in Eq (8). In fact, as demonstrated by the second panel of Fig 4, for large times one has $\delta_A^{(i,j)}(t) \simeq t^{-\alpha}$ with $\alpha < 1$, while one can show that $\log r_A^{(j-i)}(t) \simeq t^{-1}$ [25]. This means that for large enough times and any fixed l the leading contribution to the ratio of traces is given by $\delta_A^{(i,j)}(t)$, not $\log r_A^{(j-i)}(t)$. Therefore, very surprisingly, we find that translation-symmetry restoration in non-interacting systems on the lattice, and the associated quantum Mpemba effects, are *not* described the quasiparticle picture.

Scaling limit.— Although we saw that the quasiparticle picture does not describe the large time limit of a fixed subsystem, one can still wonder whether Eq (8) provides a quantitative description of symmetry restoration in a certain ‘scaling limit’, i.e., when t and l are simultaneously taken to infinity along a particular curve. The usual ‘ballistic’ scaling limit of $t, l \rightarrow \infty$ with fixed t/l produces a trivial behaviour of the Frobenius norm, which remains pinned to the initial value and shows no symmetry restoration. Remarkably, however, we find that the Frobenius distance approaches a well defined scaling form in the ‘diffusive’ scaling limit where both t and l are simultaneously taken to infinity keeping fixed $\xi = t/l^2$, see Fig. 5 (a). The latter then provides an ideal setting for investigating the predictive power of the quasiparticle picture. Noting that the scaling limit of Eq. (9) gives [25]

$$\lim_{l \rightarrow \infty} \log r_A^{(j)}(\xi l^2) = -\frac{a_j}{\xi}, \quad a_j \geq 0, \quad (12)$$

we find that the quasiparticle prediction for the scaling

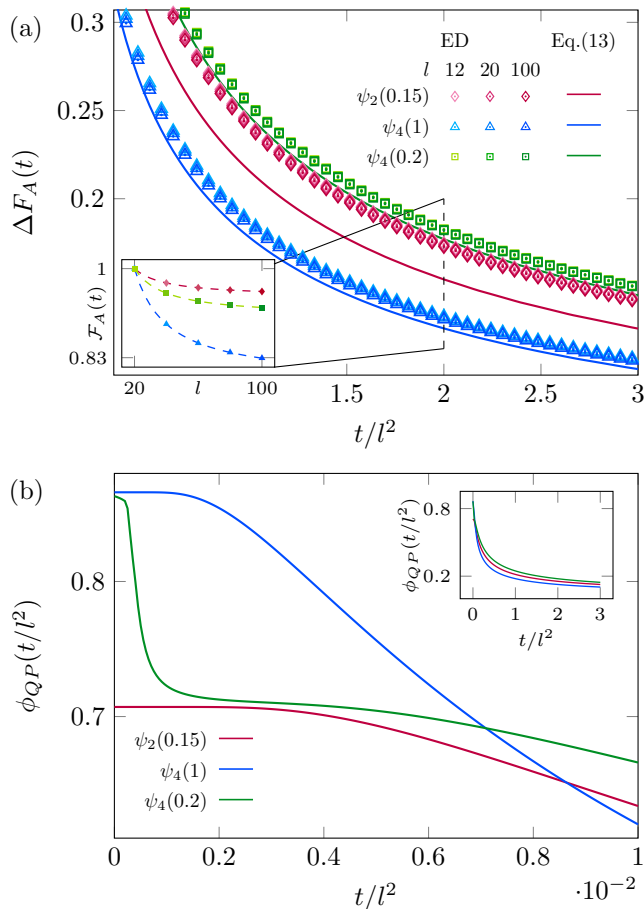


FIG. 5. The Frobenius distance in the scaling limit t/l^2 for different initial states and subsystem sizes. Plot (a) compares the method of exact diagonalisation (data points) at increasing subsystem size to the functional form Eq. (13) obtained in the $l \rightarrow \infty$ limit of the quasiparticle method (solid lines), while (b) shows Eq. (13) at earlier times. *Inset (a)*: Example, shown for $t/l^2 = 2$, of the scaling with system size compared with the prediction of Eq. (13), as defined via the normalised function $\mathcal{F}_A(t, l) = [\Delta F_A(t, l) - \phi_{QP}(\xi)] / [\Delta F_A(t, l_{min}) - \phi_{QP}(\xi)]$. The data is well described by a power-law fit of the form $a/l^b + c$, where going from top to bottom we find $a = 1.13, 2.02, 3.98$, $b = 1.02, 0.97, 1.03$, and $c = 0.95, 0.91, 0.78$. *Inset (b)*: The main plot of (b) extended to late times, showing that no further crossing occur.

form reads as

$$\phi_{QP}(\xi) = \lim_{l \rightarrow \infty} \Delta F_A(\xi l^2)|_{QP} = \sqrt{\frac{(\nu-1)}{\nu} - \frac{1}{\nu} \sum_{j=1}^{\nu-1} e^{-\frac{a_j}{\xi}}}. \quad (13)$$

This is a positive function of ξ that approaches 0 in the limit of infinite ξ , consistently describing a symmetry restoration process. This function bears explicit dependence on the initial state and, as we explicitly show in Fig. 5 (b), it can also describe quantum Mpemba effects.

To ascertain whether $\phi_{QP}(\xi)$ gives an exact description of the symmetry restoration in the scaling limit one

should once again estimate the contribution of the corrections $\delta_A^{(i,j)}(t)$. Indeed, although the latter decay in time as $t^{-\alpha}$, they can in principle grow as $l^{\alpha+\beta}$ where β is bounded from above by 1 given the sub-extensive nature of $\delta_A^{(i,j)}(t)$ in the ballistic scaling limit. Our numerical analysis suggests that $\beta = \alpha$ and, accordingly, the corrections give a finite contribution in the scaling limit: the inset of Fig. 5 shows that the difference between the rescaled ED data and $\phi_{QP}(\xi)$ does not seem to approach 0 for large l . Nevertheless, $\phi_{QP}(\xi)$ is able to at least give a qualitative description of the symmetry restoration as it captures the correct timescale and remains close to the ED data for increasing l .

Discussion.— In summary, in this paper we studied discrete translation symmetry restoration of local subsystems in the tight binding model, which can be considered the simplest example of a quantum integrable system on the lattice. We did so by computing the Frobenius distance between the reduced states of initially non-translation symmetric states and their symmetrised counterparts.

Firstly, we have seen that the symmetry restoration follows a polynomial law for large times — in contrast with the exponential one observed for random unitary circuits [21] — and can show quantum Mpemba effect for arbitrary subsystem sizes. In fact, we observed that the Frobenius distance attains a non-trivial scaling form in the ‘diffusive’ limit where time t and subsystem size l are simultaneously taken to infinity with fixed $\xi = t/l^2$.

Secondly, we have found that — although the system is trivially integrable — the symmetry restoration process goes beyond the quasiparticle picture and is described by the latter only qualitatively in the diffusive scaling limit. This means in particular that for any given l the asymptotic behaviour in time is *not* described by the quasiparticle picture. We attributed this to the discrete nature of the symmetry that is restored.

Although the quasiparticle description is only qualitative, it still gives insight into the physical mechanism behind the occurrence of quantum Mpemba effect in integrable systems. The multiplets of quasiparticles contributing to the Frobenius distance at late times are generically those with the smallest *relative* velocities between modes. This matches the physical intuition: modes moving with very similar velocity spend more time close to each other and take longer to dephase [35, 36]. The relaxation time is therefore determined by the density of modes with near-identical velocities, and by their contribution to the Frobenius distance. On the other hand, the initial value of the Frobenius distance depends on the full distribution of modes, thereby making it possible to manufacture initial states with greater initial Frobenius distance but shorter relaxation time, and vice versa, as required for QME. This mechanism generalises the one identified in Ref. [11] beyond the case of pair production and makes it obvious that QME is not just a property of the *single particle* distribution of quasiparticles, but rather of the *two-particle* one. This leads to the

conclusion that QME is a phenomenon that fundamentally goes beyond the hydrodynamic description.

We expect the phenomenology described here to be a generic feature of discrete translation symmetry restoration in integrable systems. The latter should also survive small integrability breaking terms provided that the quasiparticle lifetimes extend beyond the onset of the late-time regime (cf. Ref. [37]).

ACKNOWLEDGMENTS

We thank Katja Klobas and Colin Rylands for useful discussions. We acknowledge financial support from the Royal Society through the University Research Fellowship No. 201101 (B. B.) and from UK Research and Innovation (UKRI) under the UK government's Horizon Europe funding guarantee [grant number EP/Y036069/1] (A. G.-S.).

-
- [1] F. Ares, S. Murciano, and P. Calabrese, Entanglement asymmetry as a probe of symmetry breaking, *Nat. Commun.* **14**, 2036 (2023).
 - [2] E. B. Mpemba and D. G. Osborne, Cool?, *Phys. Educ.* **4**, 172 (1969).
 - [3] F. Ares, P. Calabrese, and S. Murciano, *The quantum mpemba effects* (2025), arXiv:2502.08087 [cond-mat.stat-mech].
 - [4] F. Ares, S. Murciano, E. Vernier, and P. Calabrese, Lack of symmetry restoration after a quantum quench: An entanglement asymmetry study, *SciPost Phys.* **15**, 089 (2023).
 - [5] S. Murciano, F. Ares, I. Klich, and P. Calabrese, Entanglement asymmetry and quantum Mpemba effect in the XY spin chain, *J. Stat. Mech.: Theory Exp.* **2024** (1), 013103.
 - [6] B. J. Khor, D. K urk uoglu, T. Hobbs, G. Perdue, and I. Klich, Confinement and kink entanglement asymmetry on a quantum ising chain, *Quantum* **8**, 1462 (2024).
 - [7] F. Ferro, F. Ares, and P. Calabrese, Non-equilibrium entanglement asymmetry for discrete groups: The example of the XY spin chain, *J. Stat. Mech.: Theory Exp.* **2024**, 023101.
 - [8] L. Capizzi and M. Mazzoni, Entanglement asymmetry in the ordered phase of many-body systems: The Ising field theory, *JHEP* **2023**, 144 (2023).
 - [9] L. Capizzi and V. Vitale, A universal formula for the entanglement asymmetry of matrix product states, *J. Phys. A: Math. Theor.* **57**, 45LT01 (2024).
 - [10] B. Bertini, K. Klobas, M. Collura, P. Calabrese, and C. Rylands, Dynamics of charge fluctuations from asymmetric initial states, *Phys. Rev. B* **109**, 184312 (2024).
 - [11] C. Rylands, K. Klobas, F. Ares, P. Calabrese, S. Murciano, and B. Bertini, Microscopic origin of the quantum Mpemba effect in integrable systems, *Phys. Rev. Lett.* **133**, 010401 (2024).
 - [12] M. Chen and H.-H. Chen, R enyi entanglement asymmetry in $(1+1)$ -dimensional conformal field theories, *Phys. Rev. D* **109**, 065009 (2024).
 - [13] M. Fossati, F. Ares, J. Dubail, and P. Calabrese, Entanglement asymmetry in CFT and its relation to non-topological defects, *J. High Energy Phys.* **2024**, 59.
 - [14] F. Caceffo, S. Murciano, and V. Alba, Entangled multiplets, asymmetry, and quantum Mpemba effect in dissipative systems, *J. Stat. Mech.: Theory Exp.* **2024** (6), 063103.
 - [15] F. Ares, S. Murciano, L. Piroli, and P. Calabrese, Entanglement asymmetry study of black hole radiation, *Phys. Rev. D* **110**, L061901 (2024).
 - [16] S. Yamashika, F. Ares, and P. Calabrese, Entanglement asymmetry and quantum Mpemba effect in two-dimensional free-fermion systems, *Phys. Rev. B* **110**, 085126 (2024).
 - [17] F. Ares, V. Vitale, and S. Murciano, The quantum Mpemba effect in free-fermionic mixed states (2024), arXiv:2405.08913.
 - [18] K. Chalas, F. Ares, C. Rylands, and P. Calabrese, Multiple crossings during dynamical symmetry restoration and implications for the quantum mpemba effect, *J. Stat. Mech.: Theory Exp.* **2024** (10), 103101.
 - [19] S. Liu, H.-K. Zhang, S. Yin, and S.-X. Zhang, Symmetry restoration and quantum Mpemba effect in symmetric random circuits, *Phys. Rev. Lett.* **133**, 140405 (2024).
 - [20] X. Turkeshi, P. Calabrese, and A. D. Luca, Quantum Mpemba effect in random circuits (2024), arXiv:2405.14514.
 - [21] K. Klobas, C. Rylands, and B. Bertini, Translation symmetry restoration under random unitary dynamics, *Phys. Rev. B* **111**, L140304 (2025).
 - [22] A. Foligno, P. Calabrese, and B. Bertini, Nonequilibrium dynamics of charged dual-unitary circuits, *PRX Quantum* **6**, 010324 (2025).
 - [23] L. K. Joshi, J. Franke, A. Rath, F. Ares, S. Murciano, F. Kranzl, R. Blatt, P. Zoller, B. Vermersch, P. Calabrese, C. F. Roos, and M. K. Joshi, Observing the quantum Mpemba effect in quantum simulations, *Phys. Rev. Lett.* **133**, 010402 (2024).
 - [24] M. Gibbins, A. Jafarizadeh, A. Gammon-Smith, and B. Bertini, Quench dynamics in lattices above one dimension: The free fermionic case, *Phys. Rev. B* **109**, 224310 (2024).
 - [25] See the Supplemental Material for: (i) the definition of the entanglement asymmetry, generalised from the simplified form of [4] for spatial symmetry breaking (ii) the explicit forms of both the normalised Frobenius distance and the $n = 2$ entanglement asymmetry for the symmetry projected state of Eq. 2.
 - [26] P. Calabrese and J. Cardy, Evolution of entanglement entropy in one-dimensional systems, *Journal of Statistical Mechanics: Theory and Experiment* **2005**, P04010 (2005).
 - [27] M. Fagotti and P. Calabrese, Evolution of entanglement entropy following a quantum quench: Analytic results for the xy chain in a transverse magnetic field, *Phys. Rev. A* **78**, 010306 (2008).
 - [28] V. Alba and P. Calabrese, Entanglement and thermodynamics after a quantum quench in integrable systems, *Proc. Natl. Acad. Sci. U.S.A.* **114**, 7947 (2017).

- [29] B. Bertini, K. Klobas, V. Alba, G. Lagnese, and P. Calabrese, Growth of Rényi entropies in interacting integrable models and the breakdown of the quasiparticle picture, *Phys. Rev. X* **12**, 031016 (2022).
- [30] B. Bertini, M. Fagotti, L. Piroli, and P. Calabrese, Entanglement evolution and generalised hydrodynamics: non-interacting systems, *Journal of Physics A: Mathematical and Theoretical* **51**, 39LT01 (2018).
- [31] Note that, at this level, a translation acts like an internal \mathbb{Z}_ν symmetry assigning charge $2j\pi/\nu$ to each mode in $[2j\pi/\nu, 2(j+1)\pi/\nu)$.
- [32] B. Bertini, F. Heidrich-Meisner, C. Karrasch, T. Prosen, R. Steinigeweg, and M. Žnidarič, Finite-temperature transport in one-dimensional quantum lattice models, *Rev. Mod. Phys.* **93**, 025003 (2021).
- [33] B. Doyon, Lecture notes on Generalised Hydrodynamics, *SciPost Phys. Lect. Notes*, 18 (2020).
- [34] A. Bastianello, B. Bertini, B. Doyon, and R. Vasseur, Introduction to the special issue on emergent hydrodynamics in integrable many-body systems, *Journal of Statistical Mechanics: Theory and Experiment* **2022**, 014001 (2022).
- [35] S. Sotiriadis, Memory-preserving equilibration after a quantum quench in a one-dimensional critical model, *Phys. Rev. A* **94**, 031605 (2016).
- [36] S. Sotiriadis, Equilibration in one-dimensional quantum hydrodynamic systems*, *Journal of Physics A: Mathematical and Theoretical* **50**, 424004 (2017).
- [37] B. Bertini and P. Calabrese, Prethermalization and thermalization in entanglement dynamics, *Phys. Rev. B* **102**, 094303 (2020).

Supplemental Material: Translation symmetry restoration in integrable systems: the noninteracting case

In this Supplemental Material, we report some results complementing the main text. In particular

- In Sec. 1 we show the explicit calculation that relates our chosen measure, the normalised Frobenius distance $\Delta F_A(\rho, t)$ of Eq. (3), to the two-point correlations of Eq. (7).
- In Sec. 2 we focus on the families of states $|\psi_2(\lambda_2)\rangle$ and $|\psi_4(\lambda_4)\rangle$ introduced in Eq. (4) and determine the constraints on the superposition parameters λ_2, λ_4 in order for QME to occur between them. These calculations are supported by our results for the Frobenius distance presented in the main text.

Appendix A: Frobenius Distance

Applying the definition of the symmetrised density matrix $\bar{\rho}_A(t)$ from Eq. (2) to Eq. (A3) yields

$$\Delta F_A(t)^2 = 1 + \frac{1}{\nu^2} \frac{\text{tr}_A \left(\sum_{i,j=0}^{\nu-1} \rho_A^{(i)}(t) \rho_A^{(j)}(t) \right)}{\text{tr}_A(\rho_A(t)^2)} - \frac{2}{\nu} \frac{\text{tr}_A \left(\sum_{j=0}^{\nu-1} \rho_A(t) \rho_A^{(j)}(t) \right)}{\text{tr}_A(\rho_A(t)^2)}. \quad (\text{A1})$$

Using that $\rho_A^{(j)}(t)$ is Gaussian for free-fermionic states, one can apply the composition rules for the trace of a product of Gaussian matrices [4] in order to rewrite the $\text{tr}_A(\rho_A^{(i)}(t) \rho_A^{(j)}(t))$ as

$$\text{tr}_A(\rho_A^{(i)}(t) \rho_A^{(j)}(t)) = \det \left[(1 - C_A^{(i)}(t))(1 - C_A^{(j)}(t)) + C_A^{(i)}(t) C_A^{(j)}(t) \right], \quad (\text{A2})$$

where $[C_A^{(j)}(t)]_{n,m} \equiv \text{tr}_A \left[c_n^\dagger c_m \rho_A^{(j)}(t) \right]$ is the correlation matrix of subsystem A under j site shifts of the *full* system.

1. Quasiparticle Solution

To proceed with the quasiparticle solution, anticipating the transform to the momentum modes of the system, we apply the approximation of Eq. (10) to Eq. (A1) and arrive at the simplified expression

$$\Delta F_A(t)^2 = \frac{1}{\nu} \left((\nu - 1) - \sum_{j=1}^{\nu-1} \frac{\text{tr}_A(\rho_A(t) \rho_A^{(j)}(t))}{\text{tr}_A(\rho_A(t)^2)} \right), \quad (\text{A3})$$

which coincides with Eq. (8) upon replacing $\rho_A(t), \rho_A^{(j)}(t)$ with their semiclassical approximations given by Eq. (5). Namely, the quasiparticle picture of $\Delta F_A(t)$ is given by the set of ν shift-dependent trace terms

$$Z_A^{(j)}(t) \equiv \text{tr}_A(\rho_A^{(0)}(t)\rho_A^{(j)}(t)). \quad (\text{A4})$$

We refer to Eq. (A4) as the *translational moments* of the system, drawing a direct analogue to the so-called *charged moments* of $U(1)$ symmetry breaking [1]. It is instructive to compare Eq. (A3) to the entanglement asymmetry $\Delta S_A^{(n)}(t)$ for $n = 2$,

$$\Delta S_A^{(n)}(t) \equiv \ln \text{tr}_A \left(\frac{\rho_A^{n+1}}{n} \right) - \ln \text{tr}_A \left(\frac{\rho_A \bar{\rho}_A^n}{n} \right) \rightarrow \quad (\text{A5})$$

$$\Delta S_A^{(2)}(t) = \ln \left[\frac{1}{\nu} \left(1 + \sum_{j=1}^{\nu-1} \frac{\text{tr}_A(\rho_A(t)\rho_A^{(j)}(t))}{\text{tr}_A(\rho_A(t)^2)} \right) \right], \quad (\text{A6})$$

since it is apparent that, following the approximation of Eq. (10), these two measures are in fact equivalent at leading order in t and l . As noted in [21], however, $\Delta S_A^{(2)}(t)$ becomes much harder to compute analytically whenever the simplification in [4] does not apply, making $\Delta F_A(t)$ our measure of choice.

Returning to the translational moments, these are computed in the quasiparticle picture by their semiclassical approximation

$$Z_A^{(j)}(t) = \prod_{k,x,\mathbf{n}} \tilde{Z}_{\mathbf{n}}^{(j)}(k) \cdot \chi_{\mathbf{n}}(A, k, x, t), \quad (\text{A7})$$

where $\tilde{Z}_{\mathbf{n}}^{(j)}(k)$ is the moment associated with the cell mode bipartition \mathbf{n} under j site shifts of the *subsystem*

$$\tilde{Z}_{\mathbf{n}}^{(j)}(k) \equiv \det \left[(1 - \tilde{C}_{\mathbf{n}}(k))(1 - \tilde{C}_{\mathbf{n}}^{(j)}(k)) + \tilde{C}_{\mathbf{n}}(k)\tilde{C}_{\mathbf{n}}^{(j)}(k) \right], \quad (\text{A8})$$

and $\chi_{\mathbf{n}}(A, k, x, t)$ is the characteristic function of cell mode bipartition \mathbf{n} with respect to the subsystem at time t

$$\chi_{\mathbf{n}}(k, x, t) = \prod_{\substack{n \in \mathbf{n} \\ \bar{n} \notin \mathbf{n}}} \chi_A(x_n(k, t)) \cdot \chi_{\bar{A}}(x_{\bar{n}}(k, t)). \quad (\text{A9})$$

Finally, using that the sum of this characteristic function over x gives the areas $\mathcal{A}_{\mathbf{n}}(A, k, t)$ associated with each cell mode bipartition, we see that the ratio function of Eq. (9) becomes

$$r_A^{(j)}(t) = \frac{Z^{(j)}(t)}{Z^{(0)}(t)} = \exp \left[\int_0^{\frac{2\pi}{\nu}} \frac{dk}{2\pi} \mathcal{A}_{\mathbf{n}}(A, k, t) \log \frac{\tilde{Z}_{\mathbf{n}}^{(j)}(k)}{\tilde{Z}_{\mathbf{n}}^{(0)}(k)} \right]. \quad (\text{A10})$$

Consequently, this solution contains all the features of a standard quasiparticle solution familiar to us from its application to the entanglement entropy [26], wherein each $\log \left(\frac{\tilde{Z}_{\mathbf{n}}^{(j)}(k)}{\tilde{Z}_{\mathbf{n}}^{(0)}(k)} \right)$ is the contribution from each cell mode bipartition to the Frobenius distance, and the set of $\mathcal{A}_{\mathbf{n}}(A, k, t)$ encodes the dynamical evolution of the cell modes with respect to subsystem A . Armed with these two ingredients, the integral over all modes k thus provides a complete picture of the evolution of the Frobenius distance reconstructed with a single $\nu \times \nu$ matrix $\tilde{C}_{\mathbf{n}}(k)$.

2. Numerical Solution

On the other hand, we can obtain the time-dependent correlations $C_A(t)$ of Eq. (A2) directly from exact diagonalisation. For purposes of generality, we consider a general superposition state

$$|\psi\rangle = \left(\prod_{j=0}^{L/\nu-1} \sum_{r=0}^{\nu-1} \alpha_r c_{\nu j-r}^\dagger \right) |0\rangle, \quad (\text{A11})$$

where α_r are the set of ν superposition parameters within each unit cell and the state is normalised as $\sum_r \alpha_r^2 = 1$. The calculation is straightforward. The two-point correlations of this initial state in position space,

$$\langle \psi | c_n^\dagger c_m | \psi \rangle = \sum_{j,r,s} \delta_{n,\nu j-r} \delta_{m,\nu j-s} \alpha_r \alpha_s^*, \quad (\text{A12})$$

yield the two-point correlations in momentum space

$$\langle \psi | c_p^\dagger c_{p'} | \psi \rangle = \left(\frac{1}{\nu} \sum_{r,s=0}^{\nu-1} e^{i(rp-sp')} \alpha_r \alpha_s^* \right) \left(\sum_{k \in \frac{2\pi}{\nu} \mathbb{Z}_\nu} \delta_{p,p'+k} \right). \quad (\text{A13})$$

This gives the time-dependent correlations, in the thermodynamic limit, as

$$[C(t)]_{n,m} \equiv \lim_{L \rightarrow \infty} \langle \psi | c_n^\dagger(t) c_m(t) | \psi \rangle = \frac{1}{\nu} \sum_{r,s=0}^{\nu-1} \int_0^{2\pi} \frac{dp}{2\pi} \sum_{k \in \frac{2\pi}{\nu} \mathbb{Z}_\nu} e^{i(n-m)p} e^{i(r-s)p} e^{i(m+s)k} e^{it[\epsilon(p-k) - \epsilon(p)]} \alpha_r \alpha_s^* \quad (\text{A14})$$

and the matrix on the subsystem $C_A(t)$ is simply obtained from the restriction $n, m \in (0, 1 \dots l)$ where $|A| \equiv l$.

Appendix B: Case Study for QME

We choose to focus on the families of states $|\psi_2(\lambda_2)\rangle$ and $|\psi_4(\lambda_4)\rangle$, defined in Eq. (4), as a means to observe QME between states of equal charge density and different symmetry breaking. In particular, λ_4 controls the $\nu = 2$ symmetry breaking of the state, with $\lambda_2 = \lambda_4 = 0$ corresponding to the Néel state and thus providing a useful benchmark whereby we can expect agreement between the solutions of these two families of states.

1. Initial Frobenius Distance

We begin with the states $|\psi_2(\lambda_2)\rangle$. The moments of Eq. (A8) are given for these $\nu = 2$ states by the two-point correlators $n_k = \langle c_k^\dagger c_k \rangle$ as

$$\tilde{Z}_{\mathbf{n}}^{(j)}(k) = |\langle \psi_k | T^j | \psi_k \rangle|^2 = |n_0 + (-1)^j n_1|^2 = \delta_{0,j} + \delta_{1,j} \left(\frac{2\lambda_2 \cos k}{1 + \lambda_2^2} \right)^2, \quad (\text{B1})$$

and we see that there is only one moment that participates,

$$\ln \tilde{Z}_{01}^{(1)}(0) = l \int_0^\pi \frac{dk}{2\pi} \ln \left(\frac{2\lambda_2 \cos k}{1 + \lambda_2^2} \right)^2 = l \ln \left(\frac{\lambda_2}{1 + \lambda_2^2} \right). \quad (\text{B2})$$

Plugging this into the Frobenius distance of Eq. (A3) then gives the initial Frobenius distance of this state as

$$\Delta F(\rho_2(\lambda_2), t = 0) = \frac{1}{2} \left[1 - \left(\frac{\lambda_2}{1 + \lambda_2^2} \right)^l \right], \quad (\text{B3})$$

where the effect of superposition is exponentially suppressed with subsystem size l . Meanwhile, the Frobenius distance of the $|\psi_4(\lambda_4)\rangle$ states must be extracted from four-point correlators, which makes dependence of the initial

Frobenius distance on λ_4 less straightforward. Instead, to prove that $\Delta F(\rho_4, t = 0) > \Delta F(\rho_2, t = 0)$, it will be sufficient for us to solve $\Delta F(\rho_4, t = 0)$ for the choices $\lambda_4 = 0$ and $\lambda_4 \rightarrow \infty$, which correspond to the minimal and maximal symmetry breaking of the state.

On the one hand, for $\lambda_4 = 0$, we have $\tilde{Z}^{(j)}(k) = \delta_{j \bmod 2, 0}$, and plugging into Eq. (A3) yields $\Delta F(\rho_4(\lambda_4), t = 0) = \sqrt{1/2}$. This coincides with the maximum value of $\Delta F(\rho_2(\lambda_2), t = 0)$ found by setting either $\lambda_2 = 0$ or $\lambda_2 \rightarrow \infty$ in Eq. (B3). On the other hand, for $\lambda_4 = \infty$, we have $\tilde{Z}^{(j)}(k) = \delta_{j, 0}$ and $\Delta F(\rho_4(\lambda_4), t = 0) = \sqrt{3/4}$. Since all other values of λ_4 correspond to intermediate symmetry breaking, we can therefore bound $\sqrt{1/2} \leq \Delta F(\rho_4(\lambda_4), t = 0) \leq \sqrt{3/4}$ and assert that $\Delta F(\rho_2(\lambda_2), t = 0) \leq \Delta F(\rho_4(\lambda_4), t = 0)$ for all λ_2, λ_4 .

2. Long-time Limit

In the $\nu = 2$ case, the only non-zero moment is

$$\tilde{Z}_{01}^{(1)}(t) = \int_0^\pi \frac{dk}{2\pi} \ln \left(\frac{2\lambda_2 \cos k}{1 + \lambda_2^2} \right)^2 \max(l - 2t \sin(k), 0). \quad (\text{B4})$$

Expanding about $k^* = 0, \pi$ to leading order in k and combining integrals, we find

$$\tilde{Z}_{01}^{(1)}(t \gg 0) = \ln \left(\frac{2\lambda_2}{1 + \lambda_2^2} \right)^2 \int_0^{l/2t} \frac{dk}{2\pi} \max(l - 2tk, 0) + O(k^2) = \ln \left(\frac{2\lambda_2}{1 + \lambda_2^2} \right)^2 \cdot \frac{l^2}{8\pi t} + O(k^2). \quad (\text{B5})$$

This causes the Frobenius distance to decay at late times as

$$\Delta F(\rho_2(\lambda_2), t \gg 0) = \left[\frac{1}{2} \left(1 - \left(\frac{2\lambda_2}{1 + \lambda_2^2} \right)^{l^2/8\pi t} \right) \right]^{1/2}, \quad (\text{B6})$$

which correctly approaches 0 from above as $t \rightarrow \infty$. Similarly, in the $\nu = 4$ case we find

$$\Delta F(\rho_4(\lambda_4), t \gg 0) = \left[\frac{1}{4} \left(3 - \Lambda_1^{l^2/8\pi t} - 2\Lambda_2^{l^2/8\pi t} \right) \right]^{1/2}. \quad (\text{B7})$$

where we have introduced $\Lambda_j = f(j)^{1/4} g(j)^{1/\sqrt{2}}$, with $\tilde{Z}_{01}^{(j)}(\pi/4) = \tilde{Z}_{23}^{(j)}(\pi/4) = g(j) + O(k)$ and $\tilde{Z}_{02}^{(j)}(\pi/4) = \tilde{Z}_{13}^{(j)}(\pi/4) = f(j) + O(k)$. From Eqs. (B6) and (B7), the second condition for QME, $\Delta F(\rho_{\nu_1}, t) < \Delta F(\rho_{\nu_2}, t)$ in the limit $t \rightarrow \infty$, can be written as

$$\frac{2\lambda_2}{1 + \lambda_2^2} \leq \Lambda_2 \Lambda_1^2. \quad (\text{B8})$$

Despite the apparent simplicity of this result, a general constraint between λ_2 and λ_4 would be too complicated to offer practical insight. Instead, we shall make the arbitrary choice to fix $\lambda_4 = 1$. This yields $f(1) = 5/9$, $f(2) = 1$, $g(1) = 21/25$ and $g(2) = 17/25$, resulting in the approximate inequalities $\lambda_2 < 0.234$ and $4.443 < \lambda_2$ for which Eq. (B8) is satisfied, and hence for which QME is observed.